Rare Met. (2024) 43(3):1275–1287
https://doi.org/10.1007/s12598-023-02493-9

RARE METALS

ORIGINAL ARTICLE

Hydrometallurgical recovery of lithium carbonate and iron phosphate from blended cathode materials of spent lithium-ion battery

Shao-Le Song, Run-Qing Liu, Miao-Miao Sun, Ai-Gang Zhen, Fan-Zhen Kong, Yue Yang*

Received: 1 November 2022 / Revised: 5 April 2023 / Accepted: 8 August 2023 / Published online: 11 December 2023

Abstract The recycling of cathode materials from spent lithium-ion battery has attracted extensive attention, but few research have focused on spent blended cathode materials. In reality, the blended materials of lithium iron phosphate and ternary are widely used in electric vehicles, so it is critical to design an effective recycling technique. In this study, an efficient method for recovering Li and Fe from the blended cathode materials of spent $LiFePO_4$ and $LiNi_xCo_yMn_{1-x-y}O_2$ batteries is proposed. First, 87% Al was removed by alkali leaching. Then, 91.65% Li, 72.08% Ni, 64.6% Co and 71.66% Mn were further separated by selective leaching with H_2SO_4 and H_2O_2. Li, Ni, Co and Mn in solution were recovered in the form of Li_2CO_3 and hydroxide respectively. Subsequently, 98.38% Fe was leached from the residue by two stage process, and it is recovered as $FePO_4{\cdot}2H_2O$ with a purity of 99.5% by precipitation. Fe and P were present in $FePO_4{\cdot}2H_2O$ in amounts of 28.34% and 15.98%, respectively. Additionally, the drift and control of various components were discussed, and cost–benefit analysis was used to assess the feasibility of potential application.

Keywords Spent lithium-ion battery; Blended cathode materials; Recovery; Lithium carbonate; Iron phosphate

S.-L. Song, R.-Q. Liu, M.-M. Sun, Y. Yang*
School of Minerals Processing and Bioengineering, Central South University, Changsha 410083, China
e-mail: Eric1911@126.com

A.-G. Zhen, F.-Z. Kong
Zhejiang Tianneng New Materials Co., Ltd., Huzhou 313103, China

1 Introduction

Lithium ion batteries (LIBs) are commonly used in small mobile devices, medium-sized electronic devices and large electric or hybrid vehicles due to their high specific energy, high working voltage and good cycle performance [1–3]. In response to the shortage of fossil fuels and the effects of climate change, countries around the world have implemented incentive policies to encourage the development of electric vehicles (EV) [4–6]. Estimates indicate that the worldwide EV stock is expected to reach at least 145 million by 2030 [7, 8]. The demand for electrochemical performance has increased as a result of the booming EV industry. Two of the most widely utilized cathode materials are lithium iron phosphate ($LiFePO_4$, LFP) and ternary ($LiNi_xCo_yMn_{1-x-y}O_2$, NCM) [9, 10]. However, LFP materials have stable cycling performance but poor rate capacity, and NCM materials have high energy density but poor safety performance [11, 12]. Thus, some scholars have begun to explore the mixed use of different materials to combine their advantages for the further improvement of performance [13, 14]. The report related to blended cathode material with excellent performance are shown in Table 1 [15–18]. Except for blended materials, Nio realized the mass production by combining LFP and NCM cells into a hybrid battery pack. It is clear that the mixed use of LFP and NCM have an important application prospect, and a large quantity of mixed spent LIBs will be produced soon. Owing to heavy metals and electrolytes, spent mixed LIBs without an appropriate treatment will inevitably cause severe risk towards the environment and resource waste [3, 19]. Therefore, efficient recycling of valuable components from spent mixed LIBs is of critical significances for pollution control and metal resource conservation.

Numerous studies have recently focused on the recycling of valuable components from spent LIBs [3, 20]. Pretreatment [21], chemical leaching, separation and regeneration [22] are generally the primary recycling techniques. Pre-treatment is adopted to separate cathode materials, anode materials, copper foil and aluminum foil [23]. Cathode materials are then used as raw materials for the recovery of various valuable metals. Chen et al. [24] explored the recycling of blended material from NMC and LFP batteries with phosphoric acid as leaching reagent. 96.3% Co, 100% Li, 98.8% Mn, 99.5% Ni and 2.7% Fe are dissolved into leaching solution, and residual components remain in the $FePO_4$ residue. $FePO_4$ was obtained after removing carbon by calcination. Obviously, this method is difficult to obtain high purity $FePO_4$ because Ni, Co and Mn cannot be completely leached. As reported [25], alkali leaching was adopted for removing Al from spent $LiFePO_4$ and $LiMn_2O_4$ cathode materials, then $LiMn_xFe_{1-x}PO_4$ can be made by ball milling and calcining with Li_2CO_3 and $NH_4H_2PO_4$ added. Despite the short process of the technique, the inconsistent lithium loss of material makes it difficult to control the lithium supplement. Li et al. [26] proposed a process for recycling spent mixed-cathode materials ($LiCoO_2$, $LiCo_{1/3}Ni_{1/3}Mn_{1/3}O_2$ and $LiMn_2O_4$). Spent cathode materials were leached with citric acid and hydrogen peroxide. The leachate was used to resynthesize new $LiCo_{1/3}Ni_{1/3}Mn_{1/3}O_2$ material by using a sol-gel method. Yang et al. [27] proposed an efficient strategy for recovering valuable metals from the high manganese leaching solution of waste mixed cathode materials. Ni and Co were first coprecipitated with sodium ethyl xanthate, and then they were separated by ammonia leaching. The remaining Mn and Li in the leachate are separated by solvent extraction. The above two methods are used to separate Ni, Co and Mn mixed materials, but they do not involve LFP. In addition, the price of the organic acid or organic salt makes it difficult to apply in large-scale recovery. To summarize, Ni, Co and Mn are simple to separate for recycling blended materials, but efficient recovery of Fe as high purity $FePO_4$ is crucial issue. Not only should the process cost be taken into consideration, but product purity should also be maintained. Therefore, it is urgent to develop a cost-effective recycling method for spent LFP and NCM blended cathode materials.

In this work, the blended cathode materials of LFP and NCM were treated by alkali leaching of Al, $H_2SO_4 + H_2O_2$ leaching of Li [20], concentrated H_2SO_4 leaching of Fe. Li_2CO_3 and $FePO_4$ were recovered by lithium-leaching solution and iron-leaching solution respectively. Besides, Ni, Co and Mn were recovered in the form of hydroxide. Finally, an effective and economical recycling method for spent blended cathode materials was proposed.

2 Experimental

2.1 Materials and reagents

The spent blended materials used in this study were provided by Zhejiang Tianneng New Material Co., Ltd, Zhejiang, China. The spent blended materials were obtained from LFP and NCM batteries by disassemble, crush and pyrolyze together with a set of pretreatment system. All the reagents, such as H_2SO_4, H_2O_2, and other, were analytical reagents purchased from Hunan Huihong Reagent Limited Corporation, and all the solutions used in this study were prepared by deionized water. The blended cathode materials contain 2.705% Ni, 1.045% Co, 6.615% Mn, 4.65% Li, 26.41% Fe and 0.291% Al, as shown in Table 2. Figure 1a shows X-ray diffraction (XRD) pattern of collected blended cathode materials. It indicates that $LiFePO_4$ and $LiNi_xCo_yMn_{1-x-y}O_2$ were mixed in the material. The morphology and element distribution of the material were analyzed according to SEM image (Fig. 1b–f). The massive particles were $LiFePO_4$ and the spherical particles were $LiNi_xCo_yMn_{1-x-y}O_2$, respectively.

2.2 Experimental procedure

2.2.1 Impurity removal

In order to obtain pure products, impurity removal was required. The main impurity in the raw material was 0.291% Al, so removal experiments of Al were conducted early in the process. According to the solubility difference between Al and other metal in NaOH solution, alkali leaching method was adopted to remove Al. 100g blended cathode materials and different concentration NaOH

Table 1 Some types of blended cathode materials related to $LiFePO_4$

No	Cathode	Advantages	Researchers
1	Blends of $LiFePO_4$ with $Li[Li_{0.17}Mn_{0.58}Ni_{0.25}]O_2$	Low cost, safety and high charge discharge rate	Whitacre et al. [15]
2	$xLi_2MnO_3(1—x)LiMO_2$ and $LiFePO_4$	High power capability and thermal stability	Gallagher et al. [16]
3	Blends of $LiFePO_4$ with $Li_3V_2(PO_4)_3$	Control capacity loss	Zheng et al. [17]
4	Coating $LiNi_{0.5}Co_{0.2}Mn_{0.3}O_2$ with $LiFePO_4$	Enhancedcapacity retention and long life	Kim [18]

Table 2 Chemical composition of spent cathode material (wt%)

Ni	Co	Mn	Li	Fe	Al	Ca	Cr	P
2.705	1.045	6.615	4.650	26.410	0.291	0.046	0.031	14.450

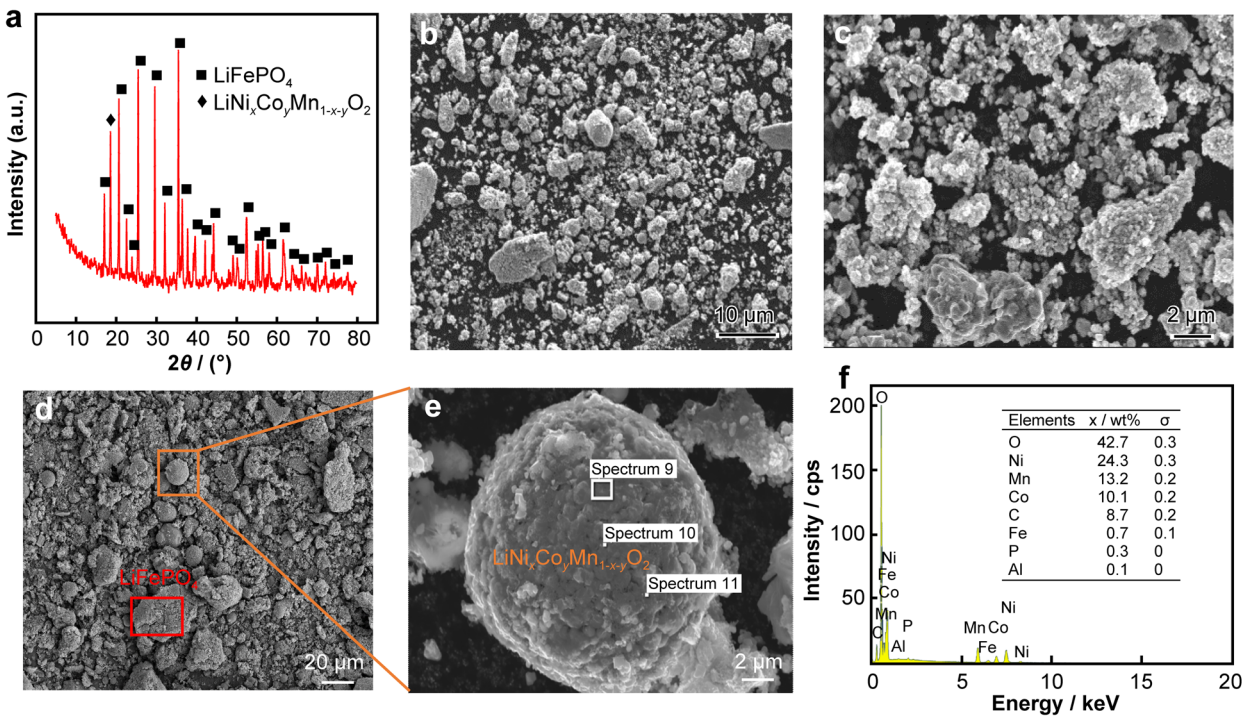

Fig. 1 **a** XRD pattern together with **b–f** SEM image of spent cathode material

solution were mixed in 1000 ml beakers. Leaching temperature was controlled by water bath pot and the slurry was stirred by mechanical agitator. The cathode materials exhibit hydrophobicity because their surfaces are coated with carbon. Slow stirring prevents leaching because the material floats on the surface of water. The slurry could easily be thrown out or onto the glass wall if the stirring speed was too fast. 300 r·min^{-1} is considered suitable, and the same was used for subsequent tests.

2.2.2 Recovery of Li_2CO_3

The residue after removing Al was further leached with H_2SO_4 and H_2O_2. The most part of Li, Ni, Co and Mn were transferred to leachate. Li_2CO_3 was recovered by precipitation from leachate after removal of Ni, Co, Mn and other metal. The leaching efficiency (E) of metal elements from waste cathode materials was calculated by Eq. (1):

$$E = \frac{c_i V}{w_i m_0} \times 100\% \quad (1)$$

where w_i (%) and m_0 (mg) are the mass fraction of element i and the total mass of raw material, respectively; c_i (mg·L^{-1}) and V (L) are the element i concentration and volume of leachate, respectively.

In the selective leaching system, H_2O_2 was used as reductant (Reaction (2)) and also oxidant (Reaction (3)).

$$H_2O_2 = O_2 + 2H^+ + 2e^- \; E_1 = -0.68 \text{ V} \quad (2)$$

$$H_2O_2 + 2H^+ + 2e^- = 2H_2O \; E_2 = 1.77 \text{ V} \quad (3)$$

where E_1 and E_2 are the standard electrode potentials of the corresponding half-reactions. Ni, Co and Mn can be reduced by H_2O_2 in leaching process, and Fe^{2+} in the $LiFePO_4$ can be converted into Fe^{3+} by H_2O_2. The reaction of leaching process can be expressed as:

$$2LiFePO_4 + H_2SO_4 + H_2O_2 \rightarrow Li_2SO_4 + 2FePO_4 \downarrow + 2H_2O \quad (4)$$

$$2Li_2Mn_2O_4 + 6H_2SO_4 + 4H_2O_2 \rightarrow 2Li_2SO_4 + 4MnSO_4 + 10H_2O + 3O_2 \uparrow \quad (5)$$

$$6LiNi_xCo_yMn_{1-x-y}O_2 + 9H_2SO_4 + 3H_2O_2 \rightarrow 3Li_2SO_4 + 6xNiSO_4 + 6yCoSO_4 + 6(1-x-y)\,MnSO_4 + 12H_2O + 3O_2\uparrow \quad (6)$$

2.2.3 Recovery of $FePO_4$

The above residue was further leached by two stages with H_2SO_4 to obtain solution containing Fe^{3+} and PO_4^{3-}. The $FePO_4$ was recovered from Fe^{3+} and PO_4^{3-} solution by neutralization precipitation. The work parameters, including reagent dosage, liquid–solid ratio, temperature, and reaction time, were optimized by single-factor experiments.

2.3 Measurement and characterization

To investigate the efficiency of leaching, the ICP-AES (FMS386, SPECTROBLUE) was used to measure the content of Li, Ni, Co, Mn, Fe and other elements in solution. The solid materials phases were characterized by X-ray diffraction (XRD, D8, Bruker Co., Ltd) at a scanning speed of 8 (°)·min^{-1} using a Cu Kα radiation. The X-ray photoelectron spectroscopy (XPS, Thermo Scientific K-Alpha) was used to analyze the phase transformation behavior of solids at a working voltage of 12 kV. The morphology and composition of the solid samples were analyzed using a scanning electron microscope (SEM, JSM-6498LV, JEOL) and energy dispersive spectrometer (EDS, Octane Prime. U.S.).

3 Results and discussion

3.1 Impurity removal

The material treated in this study contains 0.291% Al. The variables, including NaOH dosage, liquid-solid (L/S) ratio, reaction temperature and reaction time, on the effect of Al removal by alkali leaching were explored. Al metal reacting with NaOH is expressed as follows:

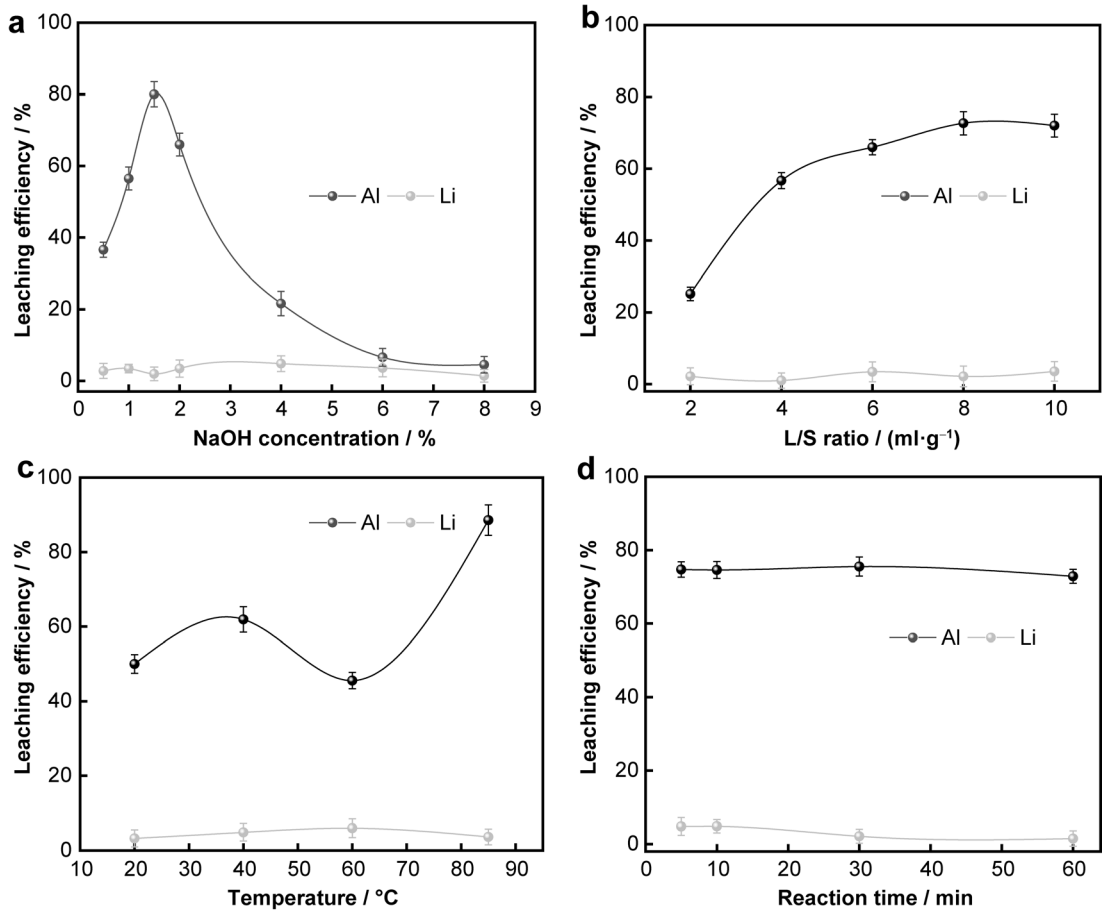

Fig. 2 Effect on leaching efficiency of **a** NaOH concentration with L/S ratio, temperature, and reaction time of 4 ml·g^{-1}, 75 °C, and 60 min, respectively; **b** L/S ratio at 4 wt% NaOH concentration, 75 °C, and 60 min; **c** temperature at 4 wt% NaOH, 4 ml·g^{-1}, and 60 min; **d** reaction time at 4 wt% NaOH, 4 ml·g^{-1} and 75 °C

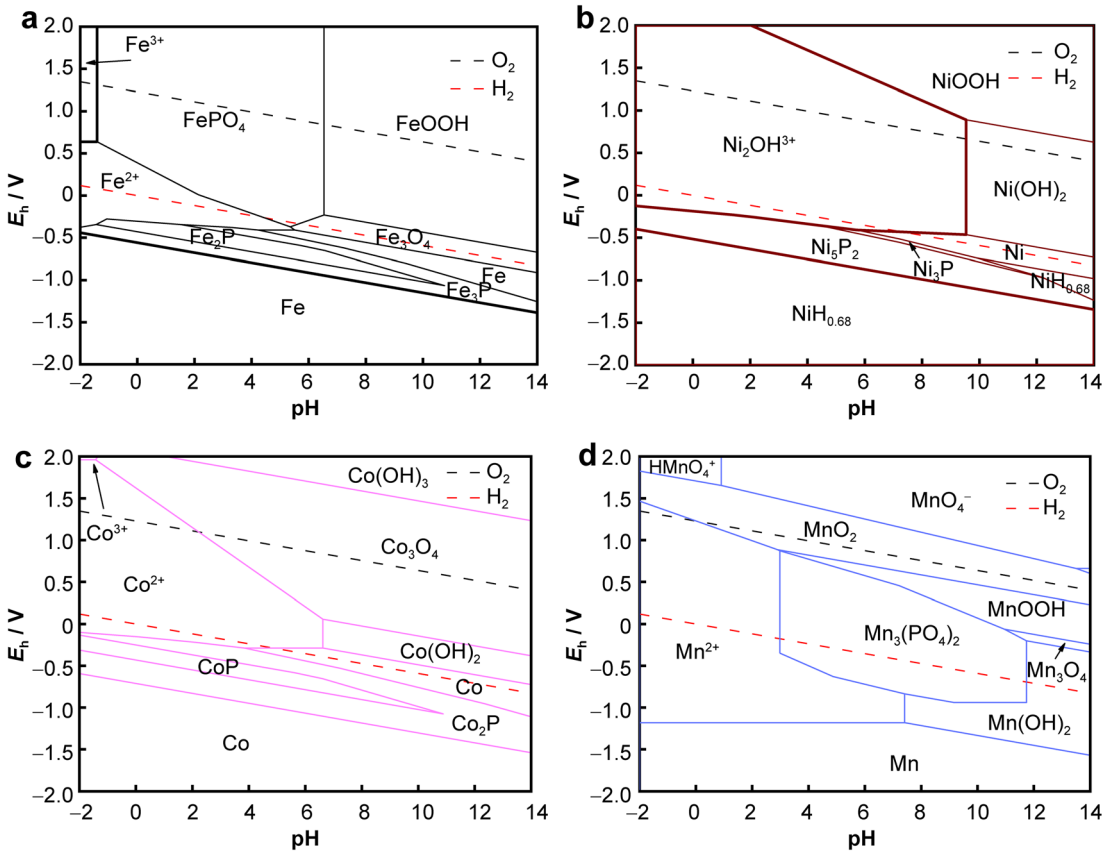

Fig. 3 E_h-pH diagram of **a** Fe-P-H_2O system, **b** Ni-P-H_2O system, **c** Co-P-H_2O system and **d** Mn-P-H_2O system

$$2Al + 2NaOH + 6H_2O \rightarrow 2Na[Al(OH)_4] + 3H_2\uparrow \quad (7)$$

The experiments with different NaOH concentration were carried out under liquid-solid ratio of 4 ml·g^{-1}, leaching temperature of 75 °C, and leaching time of 60 min. The result is depicted in Fig. 2a. It can be concluded that high leaching efficiency of Al is obtained at 1.5 wt% NaOH solution. While the leaching efficiency of Al is lower at higher NaOH concentration, because NaOH will be consumed due to the reaction with lithium iron phosphate [28]. Figure 2b shows the effect of liquid–solid ratio on Al removal efficiency under the condition of 4 wt% NaOH concentration, 75 °C, and 60 min. The leaching efficiency of Al increases with the increase of liquid-solid ratio, as can be seen. When the liquid-solid ratio is small, the slurry viscosity is large, and the raw material cannot fully contact with the reagent [29]. To reduce water consumption, liquid-solid ratio of 6 mL: g was considered to be appropriate. Figure 2c shows the effect of reaction temperature on Al removal efficiency under the conditions of 4 wt% NaOH concentration, 4 ml·g^{-1} and 60 min. Clearly, as the temperature rises, the leaching efficiency decrease first and then increase. This phenomenon may be attributed to the formation of aluminum oxide film on the surface of Al at 60 °C, and aluminum oxide film hindered the dissolution of Al in the alkaline solution. As the temperature increases to 85 °C, the oxide film is also dissolved due to the strong molecular motion [30]. Therefore, 85 °C can be selected as the optimal temperature. The effect of leaching time on the Al removal efficiency was investigated in the range of 5 to 120 min at 4 wt% NaOH concentration, 4 ml·g^{-1} and 75 °C, and the results are shown in Fig. 2d. The reaction of alkali leaching to removing Al is relatively rapid and the leaching efficiency of Al no longer changes significantly after 5min. It is worth mentioning that 1%–2% Li is leached under any conditions. This part may be attributed to the fact that Li in electrolyte is soluble in water. Based on the above experiments, the ideal conditions are 1.5 wt% NaOH concentration, 6 ml·g^{-1}, 85 °C and 5 min. Under the condition, the leaching efficiencies of Al and Li are 87% and 1.5%, respectively.

3.2 Recovery of Li_2CO_3

The E_h-pH diagrams of the Fe-P-H_2O system, Ni-P-H_2O system, Co-P-H_2O system and Mn-P-H_2O system drew by

HSC Chemistry 9.0 are shown in Fig. 3. In the E_h-pH diagrams, the top black dashed lines represent the half-reaction for the production of H_2O, and the bottom red dashed lines represent the half-reaction for the production of H_2. As shown in Fig. 3a, $FePO_4$ can remain stable over a fairly wide pH and potential range. However, Ni, Co and Mn are all in ionic state at pH below 2.5, as depicted in Fig. 3b–d. This indicated that Fe^{3+} is easier to precipitate with PO_4^{3-}, and phosphate of Ni, Co and Mn are easier to dissolve under acidic conditions.

According to thermodynamic analysis, Ni, Co and Mn can be leached by sulfuric acid, and Li is also easy to be selectively leached, but $FePO_4$ can be left in the residue due to its acid resistance, so the leaching of Li, Ni, Co and Mn are considered first. The leaching efficiencies of Li, Ni, Co, Mn and Fe under different variables, including H_2SO_4 concentration, H_2O_2 dosage, liquid-solid ratio, temperature, and leaching time, were investigated. The effect of variables on the leaching efficiency of metal elements from materials i shown in Fig. 4.

With the increase of sulfuric acid concentration, the leaching efficiencies of Li, Ni, Co, Mn and Fe witnessed an increase (Fig. 4a). However, a notable feature is that the leaching efficiency of Fe is almost kept at a lower level than other elements. The leaching of Fe can be attributed to the strong acidic environment and the lack of hydrogen peroxide [24]. The ideal concentration of H_2SO_4 is determined to be 1.4 mol·L^{-1} in order to lessen the leaching of Fe. In order to explore the effect of liquid-solid ratio on leaching, the liquid-solid ratio of 2–8 ml·g^{-1} were performed at 1.4 mol·L^{-1} H_2SO_4 concentration, 5 vol% H_2O_2 and 40 °C for 60 min respectively (Fig. 4b). With the increase of liquid-solid ratio, the leaching efficiencies increases rapidly at first and then tends to be flat. The initial increase of the leaching efficiencies could be attributed to an increase in the available surface area per unit volume of solution, and the reason for the subsequent unchanged leaching efficiencies could be attributed to the achievement of the reaction equilibrium [31, 32]. Here, in order to save water, the L/S ratio of 4 ml·g^{-1} was selected for leaching. Under the conditions of H_2SO_4 concentration of 1.4 mol·L^{-1}, H_2O_2 concentration of 5 vol%, L/S ratio of 4 ml·g^{-1}, and react time of 60 min, the effect of reaction temperature on leaching efficiency are shown in Fig. 4c. It

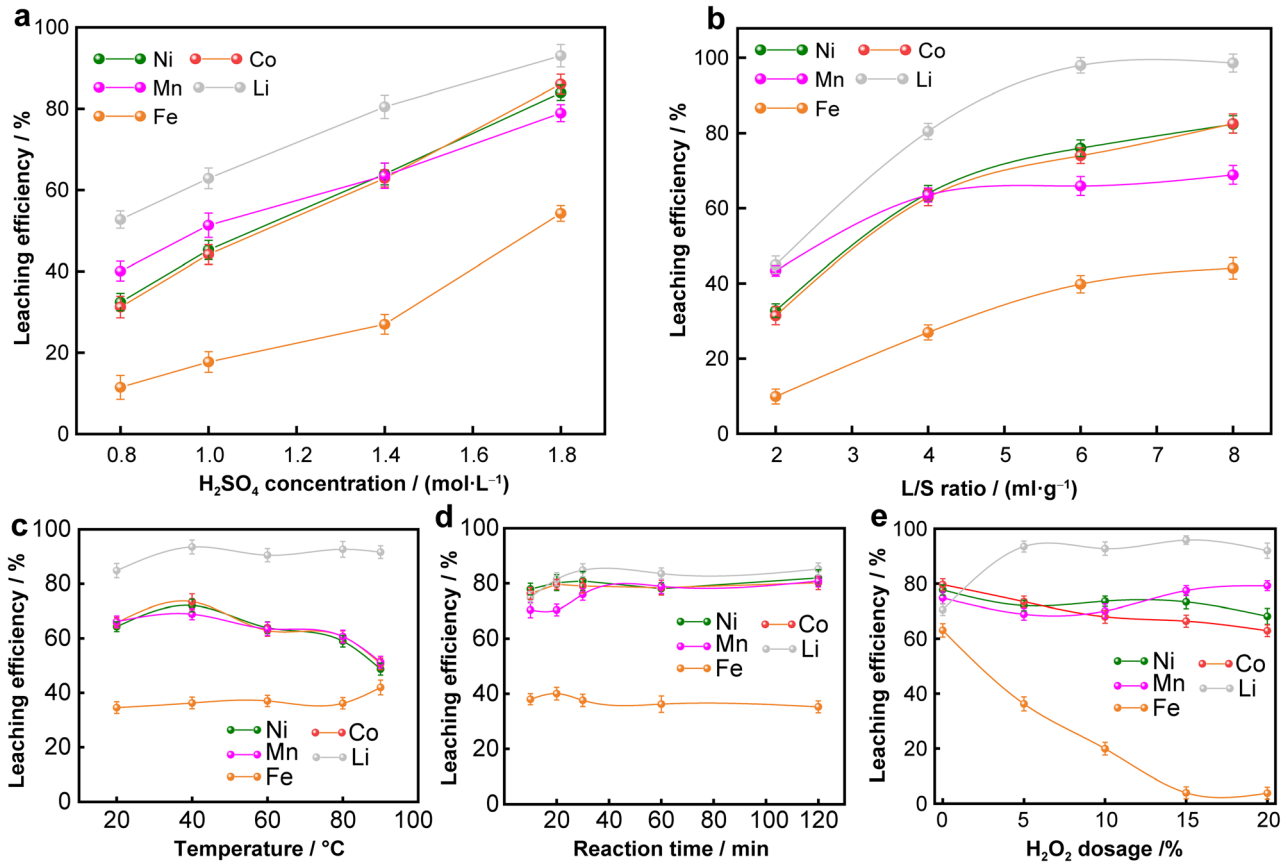

Fig. 4 Eeffect on leaching efficiency of **a** H_2SO_4 concentration at 5 vol% H_2O_2, 4 ml·g^{-1}, 60 °C and 60 min; **b** L/S ratio at 1.4 mol·L^{-1} H_2SO_4, 5 vol% H_2O_2, 60 °C, and 60 min; **c** temperature at 1.4 mol·L^{-1} H_2SO_4, 5 vol% H_2O_2, 4 ml·g^{-1}, and 60 min; **d** reaction time at 1.4 mol·L^{-1} H_2SO_4, 5 vol% H_2O_2, 4 ml·g^{-1} and 40°C; **e** H_2O_2 concentration at 1.4 mol·L^{-1} H_2SO_4, 4 ml·g^{-1}, 40 °C and 60 min

can be seen that the enhancement in the temperature from 20 to 40 °C promotes the leaching efficiencies of all metal elements. While, a further increase in the reaction temperature from 40 to 85 °C inhabits the leaching efficiencies of Ni, Co and Mn. In order to leach more Ni, Co, Mn, 40 °C can be selected as the optimal reaction temperature. As shown in Fig. 4d, reaction time has little effect on the reaction, so studying the leaching kinetics is unnecessary. H_2O_2 plays an important role during the leaching process (Fig. 4e). Without the addition of H_2O_2, the leaching efficiency of Fe is up to 63%. However, the leaching efficiency of Fe experiences a gradual decrease with the increase in the H_2O_2 dosage from 0 to 15 vol%. When the concentration of H_2O_2 is 15 vol%, the leaching efficiency of Fe is less than 2%. Under the action of H_2O_2, Fe^{2+} present in $LiFePO_4$ is oxidized to Fe^{3+} and forms $FePO_4$. This is consistent with the previous thermodynamic analysis. And it reveals that under the synergistic effect of H_2SO_4 and H_2O_2, most of the Ni, Co, Mn, and Li are leached into solution, while only a small portion of Ni, Co, Mn, Li, and almost all of the iron still remains in the leaching residue. Owing to the desire to keep Fe out of the solution as much as possible, Ni, Co, Mn, and Li are not completely leached with the small amount of acid.

In order to analyze the reaction mechanism of selective leaching process, the leaching residue was characterized. XRD pattern of the leaching residue is shown in Fig. 5a. The leaching residue is mainly composed of $FePO_4$ and $LiNi_xCo_yMn_{1-x-y}O_2$, indicating $LiFePO_4$ is oxidized to release lithium to form $FePO_4$ and $LiNi_xCo_yMn_{1-x-y}O_2$ is not completely leached. Figure 5b shows XPS spectra of Fe in residue before and after selective leaching. Before leaching, two distinct characteristic peaks at the binding energies of 710.68 and 723.48 eV mean that iron exists in the valence state of Fe^{2+}. However, the peaks move to 712.88 and 725.98 eV known as Fe^{3+} after leaching [33]. It further indicates that Fe^{2+} in material is oxidized to Fe^{3+} by H_2O_2. In Fig. 5c–e, SEM image and EDS spectrum of the leaching residue are shown. It can be seen that there are some large blocks in the leached residue. According to the content analysis, the large block has a small amount of Ni, Co, and Mn. This may be due to incomplete leaching because Ni, Co, and Mn are encased in $FePO_4$ particles.

There have been numerous previous reports on the recovery of Ni, Co, and Mn, so no systematic research has been carried out here. The synthesis of Li_2CO_3 might be the primary application for the leachate that results from selective leaching. By adding $Ca(OH)_2$ to adjust the pH value of the solution to 9–11, Ni^{2+}, Co^{2+}, Mn^{2+}, Fe^{3+} and SO_4^{2-} in the leaching solution were removed as hydroxide and sulfate. The solution was concentrated to Li concentration above 24 $g{\cdot}L^{-1}$ to increase the yield of Li_2CO_3. At

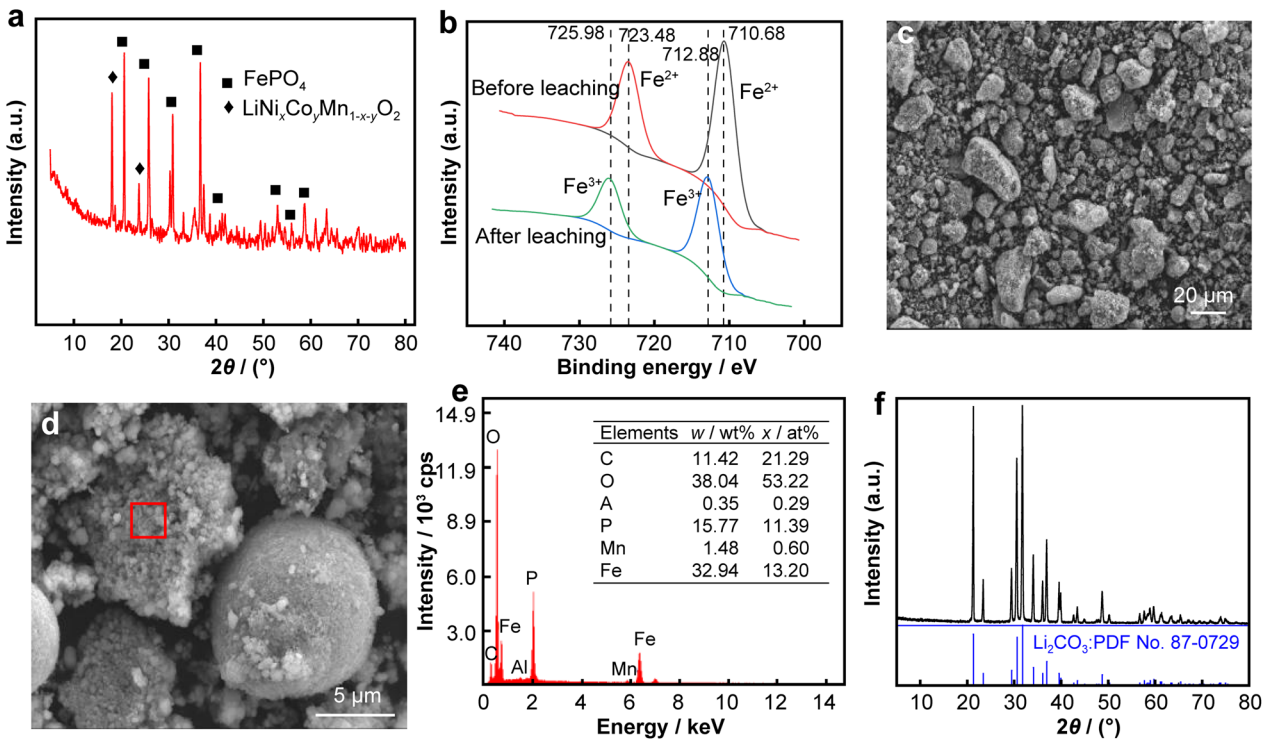

Fig. 5 **a** XRD pattern, **b** XPS spectra and **c–e** SEM image and EDS spectrum of selective leaching residue; **f** XRD pattern of Li_2CO_3 product

this point, 1.05 times the theoretical amount of Na_2CO_3 saturated solution was added to the lithium-containing concentrate to react for 1 h with stirring at 85 °C. After filtering and drying, Li_2CO_3 was eventually obtained. The precipitation reaction can be expressed as:

$$Li_2SO_4 + Na_2CO_3 \rightarrow Li_2CO_3 \downarrow + Na_2SO_4 \quad (8)$$

XRD analysis was performed for the confirmation of the synthesis product with standard card No. 87-0729 (Fig. 5 f). The elemental compositions of the Li_2CO_3 product are shown in Table 3. Na and S are the most common impurities, and Li has a mass content of 18.85% (a purity of 98.83%).

3.3 Recovery of $FePO_4$

The residue was further leached to obtain solution containing Fe with concentrated H_2SO_4. The result indicates that the leaching efficiency of Fe increases with the increase of H_2SO_4 concentration under the conditions of L/S ratio of 4 ml·g^{-1}, 40°C, 1 h (Fig. 6a). This is due to the fact that the solubility of $FePO_4$ increases as the concentration of H_2SO_4 increases and the pH value decreases. Leaching efficiency of Fe increases slowly when H_2SO_4 acid concentration exceeds 1.5 mol·L^{-1}. Given the cost, 1.5 mol·L^{-1} is chosen as the optimal H_2SO_4 concentration condition. The leaching efficiency of Fe increases with the

Table 3 Mass content of elements in Li_2CO_3 (wt%)

Al	Ca	Co	Cr	Cu	Fe	K	Li	Mg	Mn	Na	Ni	P	S
0.0005	0.0006	0.0025	0.0003	0.0004	0.0058	0.0078	18.85	0.0003	0.003	0.68	0.0014	0.0069	0.458

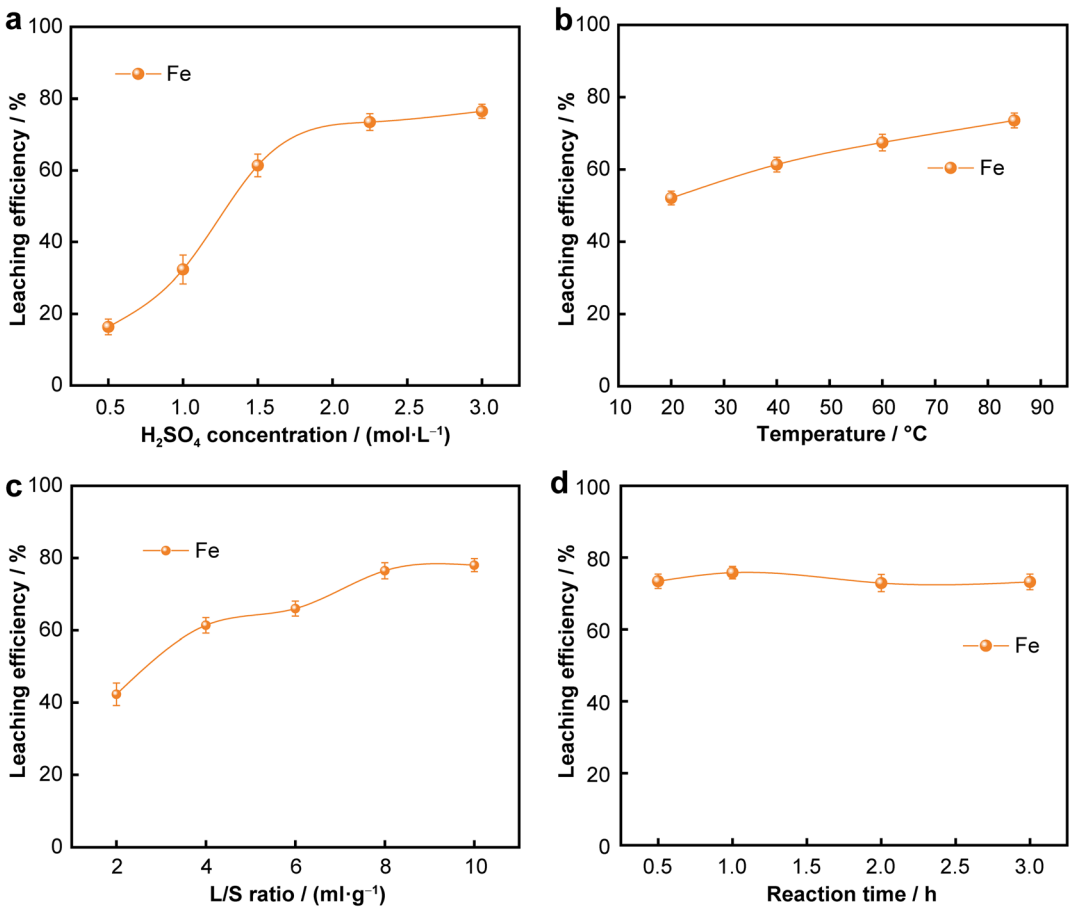

Fig. 6 Effect on leaching efficiency of **a** H_2SO_4 concentration at 4 ml·g^{-1}, 40 °C and 1 h; **b** temperature at 1.5 mol·L^{-1} H_2SO_4, 4 ml·g^{-1} and 1 h; **c** L/S ratio at 1.5 mol·L^{-1} H_2SO_4, 40 °C and 1 h; **d** reaction time at 1.5 mol·L^{-1} H_2SO_4, 4 ml·g^{-1} and 85 °C

increase of temperature (Fig. 6b), and the leaching efficiency of Fe reaches 71% at 85 °C. This indicates that the molecular collision rate is higher at higher temperatures [31]. Therefore, 85 °C was selected as optimized condition to carry out the subsequent experiment.

Under the conditions of 1.5 mol·L^{-1} H_2SO_4 concentration, 40 °C and 60 min, as depicted in Fig. 6c, the leaching efficiency of Fe increases with an increase of the L/S ratio. This is because a higher liquid-solid ratio can increase the area of contact between the material and H_2SO_4 [34]. In order to increase the concentration of Fe in the leachate, the liquid–solid ratio of 4 ml·g^{-1} was selected as the optimized condition for the subsequent experiments. The effect of time on Fe leaching is shown in Fig. 6d. The leaching results fluctuate slightly under different leaching time, but reaction time had little effect. Because the highest leaching efficiency of Fe by one-stage leaching is only 77%, there was still about 23% Fe in the leaching residue, so two-stage leaching was used to guarantee the recovery of Fe. In the second stage leaching process, Fe can be dissolved into solution with less acid than the first leaching. According to the results of the first stage leaching, the second stage leaching was carried out under the condition of L/S ratio of 3 ml·g^{-1}, 85 °C and 60 min. The effect of H_2SO_4 concentration on leaching efficiency of Fe was investigated.

According to Fig. 7a, when the H_2SO_4 concentration is 1.2 mol·L^{-1}, the leaching efficiency of Fe reaches 21.38%. Under this condition, the Fe in materials has almost been completely leached, so the leaching efficiency of Fe no longer increases when adding more H_2SO_4. It can also be seen from Table 4 that there is only 1.62% Fe and 0.66% P in the final residue, equivalent to 0.64% Fe and 0.48% P of the content of raw materials. XRD pattern of final residue is shown in Fig. 7b, and it indicates that there is no $LiFePO_4$ in the final residue. SEM images in Fig. 7c, d show that most substances remaining in the residue are carbon with particles size larger than 10 μm.

In the synthesis of $FePO_4$, the first stage leaching solution containing Fe was used as the pregnant solution. The second stage leaching solution was returned to the first stage next leaching. This can realize the reuse of acid and the accumulation of required elements. The effect of pH value on the content of impurities in $FePO_4$ product and precipitation efficiency of Fe was investigated (Fig. 8a, b)).

Table 4 Elements content of residue of two stage leaching (wt%)

Ni	Co	Mn	Li	Fe	P	Al
0.1	0.06	10.07	0.12	1.62	0.66	0.05

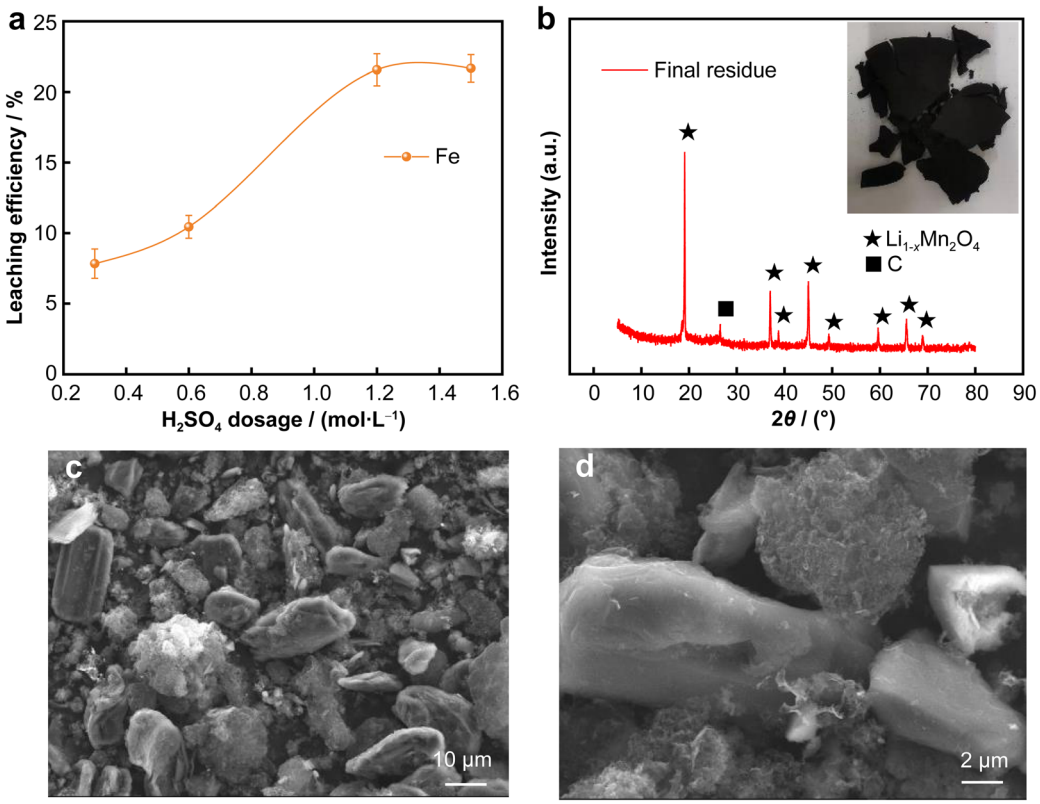

Fig. 7 **a** Effect of H_2SO_4 dosage on leaching efficiency of Fe; **b** XRD pattern and **c, d** SEM images of residue

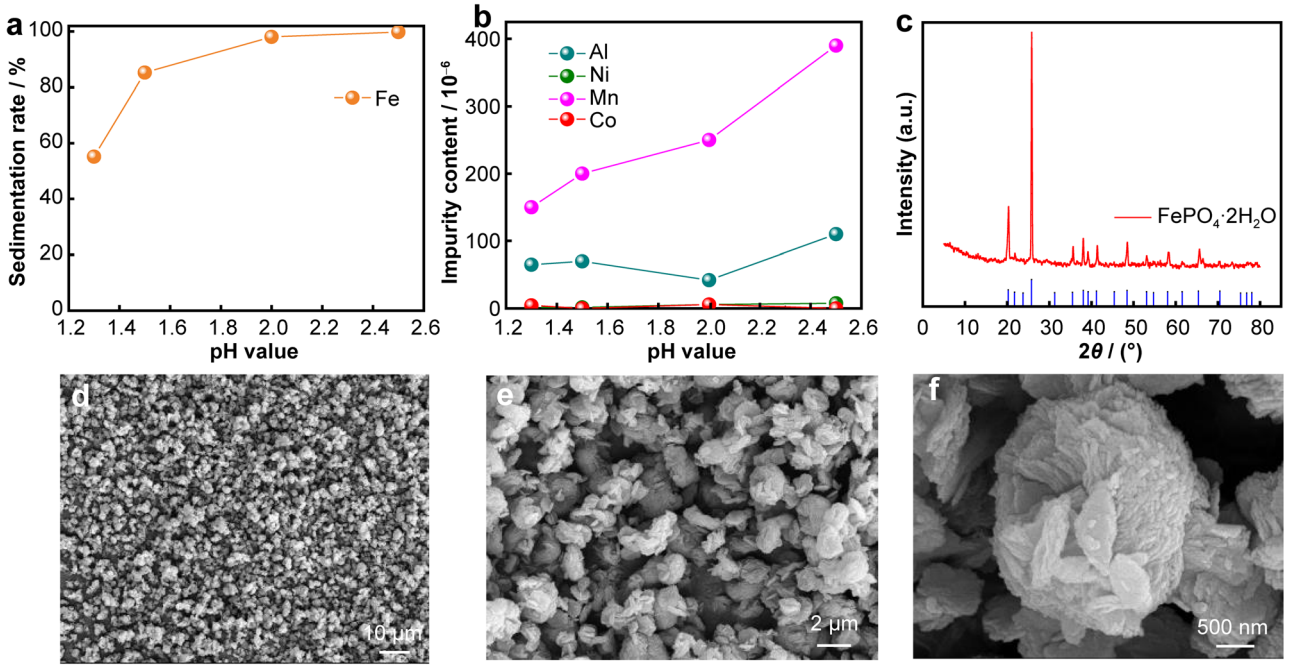

Fig. 8 **a** Effect of pH value on precipitation efficiency of Fe; **b** content of impurities in $FePO_4{\cdot}2H_2O$ product; **c** XRD pattern of $FePO_4{\cdot}2H_2O$ product;**d–f** SEM images of $FePO_4{\cdot}2H_2O$ product

Table 5 Elements content of $FePO_4$ product (wt%)

Ni	Co	Mn	Li	Ca	Na	Fe	Al	P
0.0004	0.0006	0.025	–	0.0016	0.01	28.34	0.0042	15.98

Table 6 Research report related to recycling

No	Cathode	Product	method	Refs.
1	Blend materials of LFP and NCM	LFP and NCM materials	Leaching, calcination and Precipitation	[24]
2	Blended materials of LFP and $LiMn_2O_4$	$LiMn_xFe_{1-x}PO_4$/C material	Leaching, ball milling and calcination	[25]
3	Spent LFP materials	Li_2CO_3 and $FePO_4$ residue	Mechanical ball-milling and leaching	[34]
4	Spent LFP materials	LiOH and $FePO_4$ residue	Leaching and cation-exchange	[35]
5	Blend materials of LFP and NCM	Solution containing Ni, Co, Mn, Li and $FePO_4$ residue	Leaching	[36]
6	Blend materials of LFP and NCM	Li_2CO_3, high purity $FePO_4$	Leaching and precipitation	This paper

It is obvious that with the increase of pH value, the precipitation efficiency of Fe increases gradually. When pH is 2, the precipitation is complete, and the content of Ni, Co, Mn and Al are under 0.001%, 0.001%, 0.03% and 0.01%, respectively. The components of $FePO_4$ are listed in Table 5, and the Fe: P ratio is 0.98. Figure 8d–f shows that the particle size of the $FePO_4$ product is about 2μm, and the particle size distribution is relatively uniform.

Compared with previous work, this paper emphasizes the recovery of Fe, especially in the form of high-purity $FePO_4$ (Table 6 [24, 25, 34–36]). When LFP or blended materials are recycled, only Li, Ni, Co and Mn are usually paid attention, while Fe is typically left in the residue. In any case, because of various impurities, $FePO_4$ residue is difficult to be used to regenerate high-performance LFP materials. In this paper, after removal of Al and leaching of

Ni, Co and Mn, $FePO_4$ residue is continuously leached. The solution obtained has less impurities, so that high-purity $FePO_4$ can be obtained.

3.4 Metal migration and mass balance

As depicted in Fig. 9, 87% Al was removed during the initial alkali leaching process, and during the following selective leaching, just 4.7% Al was released into the leachate. This portion of Al was removed in the separation and purification process before synthesizing Li_2CO_3, therefore there was no Al doping into finished product. After two stages of acid leaching, 7.28% Al was leached in iron leachate, leaving 1.02% Al in the final leaching residue. By controlling the synthesis conditions, the Al content in the final $FePO_4$ product is less than 0.01%, proving that the impurity can be controlled by changing the conditions.

The transition metals Ni, Co and Mn involved in this study was recovered in two parts. One portion was recovered from the lithium solution, and the other part was recovered from the solution after the synthesis of $FePO_4{\cdot}2H_2O$. Since the method for separating and recovering Ni, Co and Mn is relatively mature [37], it will not be specifically studied here.

3.5 Economic analysis

With the proposed recovery process, the economics was analyzed using a ton of blended cathode material as a sample (Table 7). The cost of raw material is ¥30,600 and total cost of reagents is 5,100. However, the total revenue generated from Li_2CO_3 and $FePO_4$ by processing a ton of blended cathode waste is ¥54,520, therefore this has a profit margin of roughly ¥18,820. The reagents used in this process are common in hydrometallurgy industry, and the high-purity products have excellent market condition. Therefore, the efficient and economic recovery of blended cathode waste is realized by this study.

4 Conclusion

In this work, the main processes included alkali leaching of Al, acid leaching of valuable metals, synthesis of Li_2CO_3

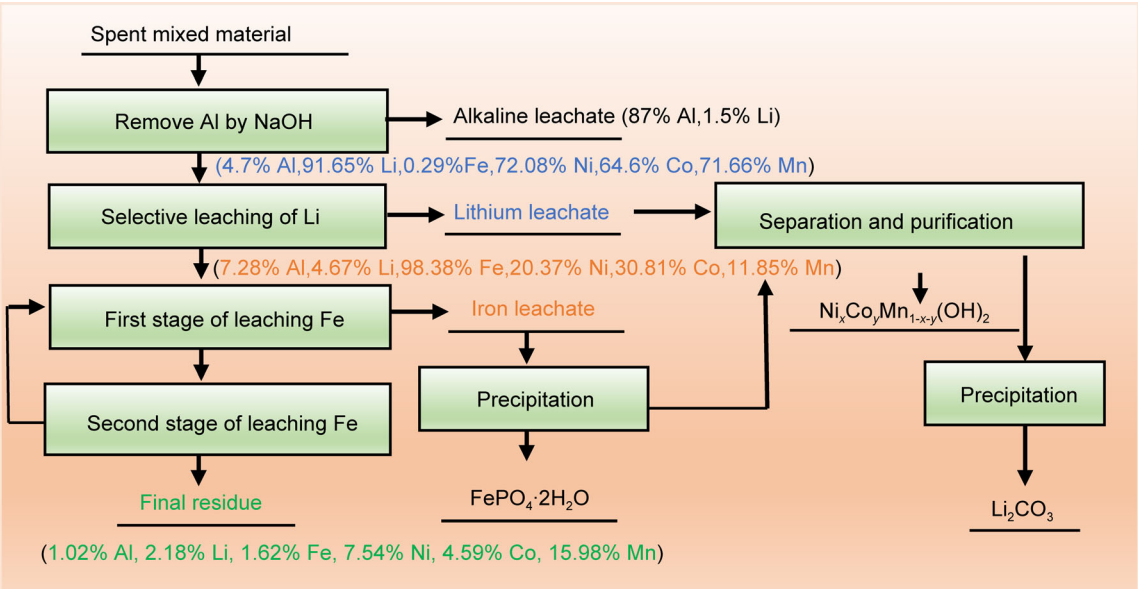

Fig. 9 Metal migration and mass balance

Table 7 Reagent consumption and profit of recycling one ton of blended materials

Items	Blended material	H_2SO_4	NaOH	H_2O_2	Na_2CO_3	Li_2CO_3	$FePO_4$	Profit
Unit price 10^3 RMB	30.6	1.2	1.5	0.6	0.4	190.0	26.0	–
Consumption or production / ton	1.000	0.700	1.700	1.050	2.70	0.198	0.650	–
Price 10^3 RMB	30.6	0.84	2.55	0.63	1.08	37.62	16.90	18.82

and $FePO_4{\cdot}2H_2O$. Under the conditions of 1.5 wt% NaOH concentration, 30 min, 85 °C and 6 $ml{\cdot}g^{-1}$, the Al removal efficiency can reach 87%. Thermodynamic analysis proves the feasibility of separating Fe and other elements. During the selective leaching process, the leaching efficiencies of Li, Ni, Co, Mn and Fe were 91.7%, 72%, 64.6%, 71.7% and 0.29% at H_2SO_4 concentration of 1.4 $mol{\cdot}L^{-1}$, H_2O_2 concentration of 15vol%, L/S ratio of 4 $ml{\cdot}g^{-1}$, temperature of 40 °C and reaction time of 60 min, respectively. The Li extraction residue is then used to continue extracting Fe with two stage leaching. Finally, Li_2CO_3 with a purity of 98.83% and $FePO_4{\cdot}2H_2O$ with a purity of 99.5% are synthesized from Li leachate and Fe leachate respectively.

This study focuses on the recovery of spent blended cathode materials by a relatively simple process, and it can provide a reference for the recycling of a large number of spent blended cathode materials in the current market.

Acknowledgements This work was financially supported by the National Key Research and Development Program (Nos. 2019YFC1907801, 2019YFC1907803 and 2019YFC1907804), the Natural Science Foundation of Hunan (Nos. 2021JJ2020066 and 2020JJ4733), the National Natural Science Foundation of China (No. 51904340) and the Central South University Innovation-Driven Research Program (No.2023CXQD009).

Declarations

Conflict of interests The authors declare that they have no conflict of interest.

References

[1] Li SN, Luo SH, Yang L, Wang Q, Zhang YH, Liu X. Synthesis and electrochemical properties of $LiFePO_4$ cathode material by ionic thermal method using eutectic mixture of tetramethyl ammonium chloride-urea. Rare Met. 2021;40(12):3477. https://doi.org/10.1007/s12598-021-01783-4.

[2] Zhang JC, Liu ZD, Zeng CH, Luo JW, Deng YD, Cui XY, Chen YN. High-voltage $LiCoO_2$ cathodes for high-energy-density lithium-ion battery. Rare Met. 2022;41(12):3946. https://doi.org/10.1007/s12598-022-02070-6.

[3] Ma LX, Chen TD, Hai CX, Dong SD, He X, Xu Q, Feng H, Xin A, Chen JT, Zhou Y. Surface engineering of Li- and Mn-rich layered oxides for superior Li-ion battery. Tungsten. 2022. https://doi.org/10.1007/s42864-022-00187-w.

[4] Li JZ. Charging Chinese future: the roadmap of China's policy for new energy automotive industry. Int J Hydr Energy. 2020;45(20):11409. https://doi.org/10.1016/j.ijhydene.2020.02.075.

[5] Hu CX, Li TR, Yuan C. Research on ordered charge and discharge of cluster electric vehicle based on index selection. 2018 2nd International Conference on Functional Materials and Chemical Engineering (ICFMCE 2018)2018. https://doi.org/10.1051/matecconf/201927201023

[6] Yi CX, Yang Y, Zhang YT, Wu XQ, Sun W, Yi LS. A green and facile approach for regeneration of graphite from spent lithium ion battery. J Clean Prod. 2020;277: 123585. https://doi.org/10.1016/j.jclepro.2020.123585.

[7] Agency IE. Global EV Outlook 2021 Technology report 2021.

[8] Jung JCY, Sui PC, Zhang JJ. A review of recycling spent lithium-ion battery cathode materials using hydrometallurgical treatments. J Energy Storage. 2021. https://doi.org/10.1016/j.est.2020.102217.

[9] Georgi-Maschler T, Friedrich B, Weyhe R, Heegn H, Rutz M. Development of a recycling process for Li-ion batteries. J Power Sour. 2012;207:173. https://doi.org/10.1016/j.jpowsour.2012.01.152.

[10] Yuan K, Ning RQ, Zhou L, Shen C, Zhou SS, Li J, Jin T, Zhang XG, Xie KY. A low-carbon strategy for revival of degraded single crystal LiNi0.6Co0.2Mn0.2O2. Rare Met. 2022;42(2):459. https://doi.org/10.1007/s12598-022-02147-2.

[11] Or T, Gourley SWD, Kaliyappan K, Yu AP, Chen ZW. Recycling of mixed cathode lithium-ion batteries for electric vehicles: Current status and future outlook. Carbon Energy. 2020;2(1):6. https://doi.org/10.1002/cey2.29.

[12] Peng JM, Chen ZQ, Li Y, Hu SJ, Pan QC, Zheng FH, Wang HQ, Li QY. Conducting network interface modulated rate performance in LiFePO4/C cathode materials. Rare Met. 2022;41(3):951. https://doi.org/10.1007/s12598-021-01838-6.

[13] Liu GW, Zhang XJ, Gong S, Jiang DP, Liu BX, Yang R, Lu SG. Phase formation and crystallization of LiMnxFe1-xPO4-C olivine material with different Mn2+ contents fabricated at lower calcination temperatures. Rare Met. 2022;41(9):3142. https://doi.org/10.1007/s12598-015-0603-5

[14] Zhong ZQ, Chen LZ, Zhu CB, Ren WB, Kong LY, Wan YX. Nano LiFePO4 coated Ni rich composite as cathode for lithium ion batteries with high thermal ability and excellent cycling performance. J Power Sour. 2020;464: 228235. https://doi.org/10.1016/j.jpowsour.2020.228235.

[15] Whitacre JF, Zaghib K, West WC, Ratnakumar BV. Dual active material composite cathode structures for Li-ion batteries. J Power Sour. 2008;177(2):528. https://doi.org/10.1016/j.jpowsour.2007.11.076.

[16] Gallagher KG, Kang SH, Park SU, Han SY. $x{Li_2MnO_3}(1–x){LiMO_2}$ blended with $LiFePO_4$ to achieve high energy density and pulse power capability. J Power Sour. 2011;196(22):9702. https://doi.org/10.1016/j.jpowsour.2011.07.054.

[17] Zheng JC, Li XH, Wang ZX, Niu SS, Liu DR, Wu L, Li LJ, Li JH, Guo HJ. Novel synthesis of $LiFePO_4$-$Li_3V_2(PO_4)_3$ composite cathode material by aqueous precipitation and lithiation. J Power Sour. 2010;195(9):2935. https://doi.org/10.1016/j.jpowsour.2009.11.006.

[18] Kim S. The reduction of formaldehyde and VOCs emission from wood-based flooring by green adhesive using cashew nut shell liquid (CNSL). J Hazard Mater. 2010;182(1–3):919. https://doi.org/10.1016/j.jhazmat.2010.03.003.

[19] Bai XT, Hu YC, Zhuang WD. Research progress on recovery and regeneration of lithium iron phosphate in spent power batteries. Chin J Rare Met. 2022;46(2):254. https://doi.org/10.13373/j.cnki.cjrm.XY20040028.

[20] Li M, Cheng LL, Yang YM, Niu F, Zhang XL, Liu DH. Development of technology for spent lithium-ion batteries recycling: a review. Chin J Rare Met. 2022,46(3):349. https://doi.org/10.13373/j.cnki.cjrm.XY20020020.

[21] Liu C, Qiu XY, Liu Y, He XJ, Chen ZQ, Liu MD. Research Status and Prospects of Physical Separation Technology of Spent Lithium-Ion Batteries. Chin J Rare Met. 2021;45(4):493. https://doi.org/10.13373/j.cnki.cjrm.XY19080040.

[22] Zhao YL, Yuan XZ, Jiang LB, Wen J, Wang H, Guan RP, Zhang JJ, Zeng GM. Regeneration and reutilization of cathode materials from spent lithium-ion batteries. Chem Eng J. 2020;383:123089. https://doi.org/10.1016/j.cej.2019.123089.

[23] Yu WH, Guo Y, Xu SM, Yang Y, Zhao YF, Zhang JJ. Comprehensive recycling of lithium-ion batteries: Fundamentals,

pretreatment, and perspectives. Energy Storage Mater. 2023;54:172. https://doi.org/10.1016/j.ensm.2022.10.033.
[24] Chen XP, Li JZ, Kang DZ, Zhou T, Ma HR. A novel closed-loop process for the simultaneous recovery of valuable metals and iron from a mixed type of spent lithium-ion batteries. Green Chem. 2019;21(23):6342. https://doi.org/10.1039/c9gc02844g.
[25] Shi HC, Zhang YB, Dong P, Huang XS, He JJ, Duan JG, Wang D, Zhang YJ. A facile strategy for recovering spent $LiFePO_4$ and $LiMn_2O_4$ cathode materials to produce high performance $LiMn_xFe_{1-x}PO_4$/C cathode materials. Ceram Int. 2020;46(8):11698. https://doi.org/10.1016/j.ceramint.2020.01.201.
[26] Li L, Bian YF, Zhang XX, Guan YB, Fan ES, Wu F, Chen RJ. Process for recycling mixed-cathode materials from spent lithium-ion batteries and kinetics of leaching. Waste Manage. 2018;71:362. https://doi.org/10.1016/j.wasman.2017.10.028.
[27] Yang Y, Liu FH, Song SL, Tang HH, Ding ST, Sun W, Lei SY, Xu SM. Recovering valuable metals from the leaching liquor of blended cathode material of spent lithium-ion battery. J Environ Chem Eng. 2020;8:104358. https://doi.org/10.1016/j.jece.2020.104358.
[28] Ferreira DA, Prados LMS, Majuste D, Mansur MB. Hydrometallurgical separation of aluminium, cobalt, copper and lithium from spent Li-ion batteries. J Power Sour. 2009;187(1):238. https://doi.org/10.1016/j.jpowsour.2008.10.077.
[29] Li GH, Gu FQ, Jiang T, Luo J, Deng BN, Peng ZW. Beneficiation of aluminum-, Iron-, and titanium-bearing constituents from diasporic bauxite Ores. Jom. 2017;69(2):315. https://doi.org/10.1007/s11837-016-2215-4.
[30] Da Costa AJ, Matos JF, Bernardes AM, Muller IL. Beneficiation of cobalt, copper and aluminum from wasted lithium-ion batteries by mechanical processing. Int J Miner Proc. 2015;145:77. https://doi.org/10.1016/j.minpro.2015.06.015.
[31] Chen WS, Ho HJ. Recovery of valuable metals from lithium-ion batteries NMC cathode waste materials by hydrometallurgical methods. Metals. 2018;8(5):321. https://doi.org/10.3390/met8050321.
[32] Jha MK, Kumari A, Jha AK, Kumar V, Hait J, Pandey BD. Recovery of lithium and cobalt from waste lithium ion batteries of mobile phone. Waste Manage. 2013;33(9):1890. https://doi.org/10.1016/j.wasman.2013.05.008.
[33] Chen BB, Liu M, Cao S, Chen GR, Guo XW, Wang XY. Regeneration and performance of $LiFePO_4$ with Li_2CO_3 and $FePO_4$ as raw materials recovered from spent $LiFePO_4$ batteries. Mater Chem Phys. 2022;279:125750. https://doi.org/10.1016/j.matchemphys.2022.125750.
[34] Zheng XH, Gao WF, Zhang XH, He MM, Lin X, Cao HB, Zhang Y, Sun Z. Spent lithium-ion battery recycling – Reductive ammonia leaching of metals from cathode scrap by sodium sulphite. Waste Manage. 2017;60:680. https://doi.org/10.1016/j.wasman.2016.12.007.
[35] Zhang QY, Fan E, Lin J, Sun SS, Zhang XD, Chen RJ, Wu F, Li L. Acid-free mechanochemical process to enhance the selective recycling of spent $LiFePO_4$ batteries. J Hazard Mater. 2023;443:130160. https://doi.org/10.1016/j.jhazmat.2022.130160.
[36] Li Z, He LH, Zhu YF, Yang C. A green and cost-effective method for production of LiOH from spent $LiFePO_4$. ACS Sustain Chem Eng. 2020;8(42):15915. https://doi.org/10.1021/acssuschemeng.0c04960.
[37] Xu ZD, Dai Y, Hua D, Gu HN, Wang N. Creative method for efficiently leaching Ni Co, Mn, and Li in a mixture of $LiFePO_4$ and $LiMO_2$ using only Fe(III). ACS Sustain Chem Eng. 2021;9(11):3979. https://doi.org/10.1021/acssuschemeng.0c09207.
[38] Chen JQ, Zhang HP, Zeng ZY, Gao Y, Liu CH, Sun XQ. Separation of lithium and transition metals from the leachate of spent lithium-ion battery by extraction-precipitation with p--tert-butylphenoxy acetic acid. Hydrometallurgy. 2021;206:105768. https://doi.org/10.1016/j.hydromet.2021.105768.